Jurnal Mekanikal
December 2007, No. 24, 68 - 79

TWO-PHASE FLOW SIMULATION WITH LATTICE BOLTZMANN METHOD

Nor Azwadi Che Sidik*, Takahiko Tanahashi

*Faculty of Mechanical Engineering,
Universiti Teknologi Malaysia,
81310 Skudai, Johor Bahru

School for Open and Environmental System,
Keio University,
223-0061 Yokohama, Japan

ABSTRACT

This paper concerned with the simulation of two phase fluid flows in two dimensions using lattice Boltzmann method. The original free energy lattice Boltzmann model is reviewed in some detail. Which was then developed into a new free energy model based on the isotropy approach and The Gallilean invariance is also considered. Some simulation results, which have been performed elsewhere, are repeated to test the validity of this model.

Keywords: *Lattice Boltzmann method, free energy, Gallilean invariance, bubble coalesce, bubble motion*

1.0 INTRODUCTION

The importance of understanding fluid flow with a change in phase arises from the fact that many industrial processes rely on these phenomena for materials processing or for energy transfer, e.g. petroleum processing, paper-pulping, power plants and boiling water reactor. There are many common examples of multiphase flow not only in industrial processes but also everyday life. Thus the understanding of multiphase flow is essential for both fundamental research and engineering applications. However, due to the complex nature of multiphase flow, theoretical solutions are generally limited to relatively simple cases. Meanwhile, the experimental approaches for multiphase flow are very expensive if not impossible, depending on the scale and/or fluid composition. Therefore, it is reasonable to say that numerical simulations are primarily useful in studying the underlying physics of multiphase flow and providing information about the details of processes that are difficult to obtain by theoretical analysis or by experiments.

Recently, simulating multiphase flow with Lattice Boltzmann Method (LBM) has attracted much attention. Microscopically, the phase segregation and surface tension in multiphase flow are because of the interparticle forces/interactions. Due

* Corresponding author: E-mail: azwadi@fkm.utm.my

to its kinetic nature, the LBM is capable of incorporating these interparticle interactions, which are difficult to implement in traditional methods.

In general there are three types of lattice Boltzmann models have been advanced to simulate multiphase flow systems. The first type is the so-called colored model for immiscible two-phase flow proposed by Gunstensen et al. [1]. Gunstensen et al used colored particles to distinguish between phases. The color model was further developed by later studies [2], but it has serious limitations. One of the most significant problems is that the model is not rigorously based upon thermodynamics, so it is difficult to incorporate microscopic physics into the model [3].

The second type of lattice Boltzmann (LB) approach to model multi-component fluids was derived by Shan and Chen (SC model) [4]. In the SC model, a non-local interaction force between particles at neighboring lattice sites is introduced. The net momentum, modified by interparticle forces, is not conserved by the collision operator at each local lattice node, yet the system's global momentum conservation is exactly satisfied when boundary effects are excluded [5]. The main drawback of the SC model, however, is that it is not well-established thermodynamically. One can not introduce temperature since the existence of any energy-like quantity is not known [6].

The third type of LB model for multiphase flow is based on the free-energy (FE) approach, developed by Swift et al. [7], who imposed an additional constraint on the equilibrium distribution functions. The FE model conserves mass and momentum locally and globally, and it is formulated to account for equilibrium thermodynamics of nonideal fluids, allowing for the introduction of well defined temperature and thermodynamics. The major drawback of the FE approach is the unphysical non-Galilean invariance for the viscous terms in the macroscopic Navier-Stokes equation. Efforts have been made to restore the Galilean invariance to second-order accuracy by incorporating the density gradient terms into the pressure tensor [8, 9].

In the present work, the free energy approach of multiphase lattice Boltzmann scheme proposed by Yonetsu [9] is used to simulate two-phase flow phenomena. Yonetsu has shown that his model could predict well the bubble shear phenomena and obtained a very good agreement with analytical result for the Laplace`s law pressure of droplet-gas system. As extension to their works, we include the external force in the governing equation and simulate the bubble rises phenomenon.

This paper is organized as follows. In Section 2, a brief overview of lattice Boltzmann method along with theory of free-energy multiphase lattice Boltzmann is discussed. The isotherms P vs V graph from Van-Der Waals fluid equation is plotted in order to find the value of density for both liquid and gas phases at certain pressure and temperature. In Section 3 two-phase at initially non-equilibrium condition, bubbles rise and coalesce phenomena were simulated to show capability of the two-phase lattice Boltzmann model. The final section concludes this study.

2.0 MULTIPHASE LATTICE BOLTZMANN METHOD

The starting points for lattice Boltzmann simulations is the evolution equation, discrete in space and time, for a set of distribution functions f_i. If a two-dimension nine-velocity model (D2Q9) is used, then the evolution equation for a given f_i take the form

$$f_i(\mathbf{x}+\mathbf{e}_i\Delta t, t+\Delta t)-f_i(\mathbf{x},t)=\frac{1}{\tau}\left[f_i(\mathbf{x},t)-f_i^{eq}(\mathbf{x},t)\right]+F \tag{1}$$

where Δt is the time step, $\mathbf{e}$ is the particle's velocity, τ is the relaxation time for the collision, F is the external force and $i = 0, 1,\ldots, 8$. Noted that the first term in the right hand side of Equation 1 is the collision term where the BGK approximation [10] has been applied. The discrete velocity is expressed as $\mathbf{e}_i = (0, 0)$ for $i = 0$, $\mathbf{e}_i = (\cos(i-1)\pi/4, \sin(i-1)\pi/4)$ for $i = 1, 3, 5, 7$ and $\mathbf{e}_i = 2^{1/2}(\cos(i-1)\pi/4, \sin(i-1)\pi/4)$ for $i = 2, 4, 6, 8$. f_i^{eq} is an equilibrium distribution function, the choice of which determines the physics inherent in the simulation.

The updating of the lattice consists of basically two steps: a streaming process, where the particle densities are shifted in discrete time steps through the lattice along the connection lines in direction $\mathbf{e}_i$ to their next neighboring nodes and a collision step, where locally a new particle distribution is computed by evaluating the right hand side of Equation 1.

In free-energy two-phase lattice Boltzmann model, the equilibrium distribution determines the physics inherent in the simulation. A power series in the local velocity is assumed [11]

$$f_i^{eq} = A + B(e_{i,\alpha}u_\alpha)+C(e_{i,\alpha}e_{i,\beta}u_\alpha u_\beta)+Du^2+G_{\alpha\beta}e_{i,\alpha}e_{i,\beta} \tag{2}$$

where the summation over repeated Cartesion indices is understood. The coefficients A, B, C, D and $G_{\alpha\beta}$ are determined by placing constraint on the moments of f_i^{eq}. In order that the collision term conserves mass and momentum, the first moments of f_i^{eq} are constrained by

$$\sum_i f_i^{eq} = \rho \tag{3}$$

$$\sum_i e_{i,\alpha} f_i^{eq} = \rho u_\alpha \tag{4}$$

The next moment of f_i^{eq} is chosen such that the continuum macroscopic equations approximated by evolution equation correctly describe the hydrodynamics of a one-component, non-ideal fluid. This gives

$$\sum_i e_{i,\alpha}e_{i,\beta}f_i^{eq} = P_{\alpha\beta} + \rho u_\alpha u_\beta + \upsilon\left[u_\alpha\partial_\beta(\rho)+u_\beta\partial_\alpha(\rho)+u_\gamma\partial_\gamma(\rho)\delta_{\alpha\beta}\right] \tag{5}$$

where $\upsilon = c^2(\tau - 1/2)\Delta t/3$is the kinematic shear viscosity and $P_{\alpha\beta}$ is the pressure tensor. In order to fully contrain the coefficients A, B , C , D and $G_{\alpha\beta}$, a fourth condition is needed, which is

$$\sum_i e_{i,\alpha} e_{i,\beta} e_{i,\gamma} f_i^{eq} = \frac{\rho c^2}{3}\left(u_\alpha \delta_{\beta\gamma} + u_\beta \delta_{\alpha\gamma} + u_\gamma \delta_{\alpha\beta}\right) \tag{6}$$

The values of the coefficients can be determined by a well established procedure. For the constraints (Equations 3-6) one possible choice of coefficients is:

$$A_1 = 4A_2,\ A_0 = \rho - 4(A_1 + A_2) - \frac{3}{2c^2}\left[2\upsilon u_\gamma \partial_\gamma \rho + \kappa(\partial_\gamma \rho)^2\right] \tag{7}$$

$$A_2 = \frac{1}{12c^2}\left[p_0 - \kappa(\partial_\gamma \rho)^2 - \kappa\rho\partial_{\gamma\gamma}\rho\right] \tag{8}$$

$$B_2 = \frac{\rho}{12c^2},\ B_1 = 4B_2 \tag{9}$$

$$C_2 = \frac{\rho}{8c^4}, C_1 = 4C_2 \tag{10}$$

$$D_2 = -\frac{\rho}{24c^2}, D_1 = 4D_2,\ D_0 = -\frac{2\rho}{3c^2} \tag{11}$$

$$G_{2xx} = \frac{1}{8c^4}\left[2\upsilon u_x \partial_x \rho + \kappa(\partial_x \rho)^2\right] \tag{12}$$

$$G_{2xy} = G_{2yx} = \frac{\upsilon}{8c^4}\left(u_x \partial_y \rho + u_y \partial_x \rho\right) + \frac{\kappa}{8c^4}(\partial_x \rho)(\partial_y \rho) \tag{13}$$

$$G_{2yy} = G_{2xx} \tag{14}$$

$$G_{1\alpha\beta} = 4G_{2\alpha\beta} \text{ for all } \alpha, \beta \tag{15}$$

The analysis of Holdych et al. [8] shows that the evolution scheme, Equation 1 approximates the continuity equations

$$\partial_t \rho + \partial_\alpha(\rho u_\alpha) = 0 \tag{16}$$

and the following Navier-Stokes level equation:

$$\partial_t(\rho u_\alpha)+\partial_\beta(\rho u_\alpha u_\beta)=-\partial_\beta P_{\alpha\beta}+\upsilon\partial_\beta\left[\rho\left\{\partial_\beta u_\alpha+\partial_\alpha u_\beta+\delta_{\alpha\beta}\partial_\gamma u_\gamma\right\}\right]$$
$$-\frac{3\upsilon}{c^2}\partial_\beta\left[u_\alpha\partial_\gamma P_{\beta\gamma}+u_\beta\partial_\gamma P_{\alpha\gamma}+\partial_\gamma\left(\rho u_\alpha u_\beta u_\gamma\right)\right]$$
$$-\frac{3\upsilon}{c^2}\partial_\beta\left[\left(\partial_\beta P_{\alpha\beta}\right)\left(\partial_\gamma\rho u_\gamma\right)\right]$$
$$-\frac{3\upsilon}{c^2}\partial_\beta\left[u_\alpha\partial_\gamma\left(u_\beta\partial_\gamma\rho+u_\gamma\partial_\beta\rho+\delta_{\gamma\beta}u_\lambda\partial_\lambda\rho\right)\right]$$
$$-\frac{3\upsilon}{c^2}\partial_\beta\left[u_\beta\partial_\gamma\left(u_\alpha\partial_\gamma\rho+u_\gamma\partial_\alpha\rho+\delta_{\alpha\gamma}u_\lambda\partial_\lambda\rho\right)\right]$$
$$+\frac{3\upsilon}{c^2}\partial_\beta\left[\partial_t\left(u_\alpha\partial_\beta\rho+u_\beta\partial_\alpha\rho+\delta_{\alpha\beta}u_\gamma\partial_\lambda\rho\right)\right] \tag{17}$$

The top line is the compressible Navier-Stokes equation while the subsequent lines are error terms. We have, then, described a framework for a one component free energy lattice Boltzmann.

The theory of Van-Der Waals fluid is very close related to the multiphase phenomena. The Van Der Waals equation of state is can be written as

$$\left(p+\frac{n^2a}{V^2}\right)(\mathrm{V}-\mathrm{nb})=nRT \tag{18}$$

where n is the mole number, a and b are constant characteristic of a particular gas and R is the gas constant. p, V and T are as usual the pressure, volume and temperature. Equation 18 can be rewritten in terms of the following 'reduced' quantities

$$\left(\tilde{p}+\frac{3}{\tilde{V}}\right)\left(3\tilde{V}-1\right)=8\tilde{T} \tag{19}$$

where

$$V_C=3b,\ T_C=\frac{8a}{27bR},\ p_C=\frac{8a}{27b^2} \tag{20}$$

and

$$\tilde{p}=\frac{p}{p_C},\ \tilde{V}=\frac{V}{V_C},\ \tilde{T}=\frac{T}{T_C} \tag{21}$$

Figure 1 shows plot of isotherms on a $\tilde{p}-\tilde{V}$ diagram for various $\tilde{T}$. For $\tilde{T}>1$, the graph looks very much like the ideal gas isotherms. However, for $\tilde{T}<1$, a 'loop' (minimum and maximum) in $\tilde{p}$ is occur. At this condition, the system separates

into two phases, a gas of volume V_G and a liquid of volume V_L. The two coexisting phases both have the same pressure denoted by P_{LG}. The value of V_G and V_L can be determined by recalling that at equilibrium condition, the chemical potentials of the two phases must be equal. As a result we come out with the situation that they can be found geometrically by the so called 'Maxwell equal area construction' as shown in the Figure 1. For Example, for the value of $T = 0.55$, the value of V_G and V_L are 0.4523 (or density ρ_G = 2.221), and 0.2043 (or density ρ_L = 4.895) respectively.

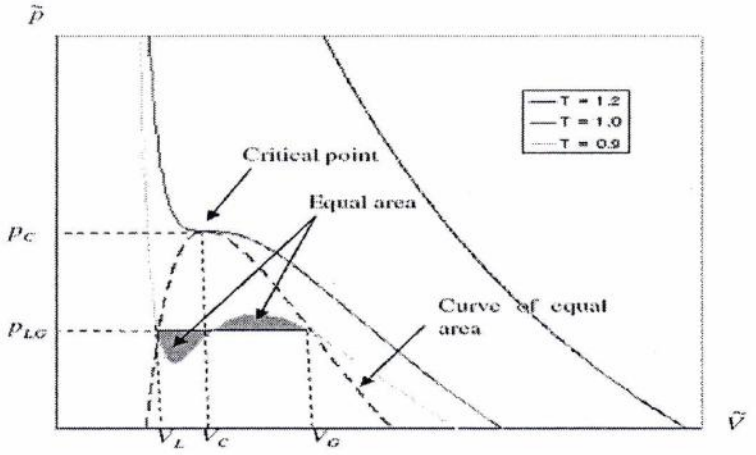

Figure 1: Isotherms plot of $\tilde{p} - \tilde{V}$

The thermodynamics of the fluid enters the lattice Boltzmann simulation via pressure tensor $P_{\alpha\beta}$. The equilibrium properties of a system with no surface (i.e periodic boundaries) can be described by a Landau free energy functional

$$\Psi = \int dV \left[\psi(\rho, T) + \frac{\kappa}{2} (\partial_\alpha \rho)^2 \right] \tag{22}$$

subject to the constraint

$$M = \int dV \rho \tag{23}$$

where $\psi(\rho, T)$ is the free energy density of bulk phase, κ is a constant related to the surface tension, M is the total mass of fluid and the integrations are over all space. The second term in Equation 22 gives the free energy contribution from density gradients in an inhomogeneous system. For Van-Der Waals fluid, free energy density of bulk phase can be written in the form

$$\psi(\rho, T) = \rho RT \ln\left(\frac{\rho}{1 - b\rho}\right) - a\rho^2 \tag{24}$$

Introducing a constant Lagrange multiplier, μ, we can minimise Equation 22, giving a condition for equilibrium as

$$\frac{\partial \psi}{\partial \rho} - \mu - \kappa \nabla^2 \rho = 0 \tag{25}$$

By multiplying Equation 25 by $\partial\rho/\partial x$ and integrating once with respect to x, we obtain the first integral

$$\psi - \mu\rho - \frac{\kappa}{2}(\partial_\alpha \rho)^2 = \text{const.} \tag{26}$$

At equilibrium condition, the chemical potential and pressure of both phases are given by

$$\mu = RT \ln\left(\frac{\rho}{1-b\rho}\right) + \frac{RT}{1-b\rho} - 2a\rho \tag{27}$$

$$p = \frac{\rho RT}{1-b\rho} - a\rho^2 \tag{28}$$

respectively. We now define $W(\rho, T) = \psi - \mu\rho + p$, meaning that Equation 25 and Equation 26 can be rewritten as

$$\frac{\partial W}{\partial \rho} = \kappa \nabla^2 \rho \tag{29}$$

$$W = \frac{\kappa}{2}(\partial_\alpha \rho)^2 \tag{30}$$

By solving Equation 30, we are able to determine the density profile at the interface for different values of κ as shown in Figure 2. Noted that fourth order Rungge-Kutta scheme is used to solve Equation 30 and temperature is set at $T = 0.55$. As can be seen from the graph, the value of κ is related to the density gradient at the interface and also affects the width of interface.

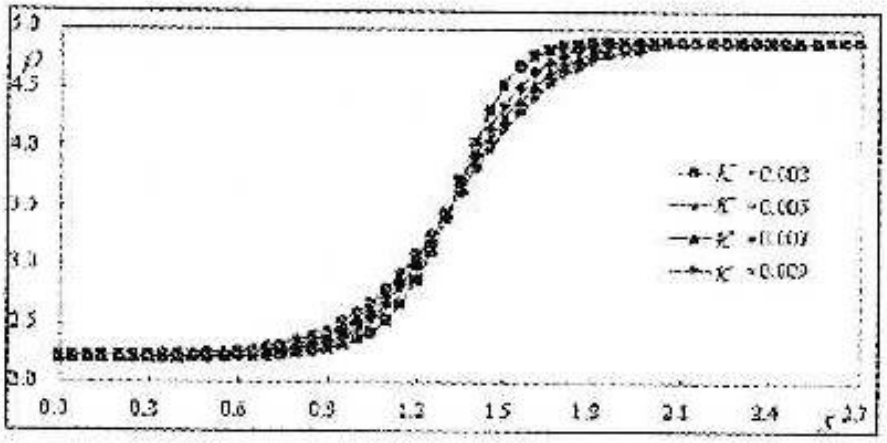

Figure 2: Density gradient at the interface for various value of κ

3.0 SIMULATION RESULTS

3.1 Phase Separation

In this section, the phase separation which is based from the thermodynamic instability of the Van-Der Waals fluid is simulated. As discussed in Section 2.0, if the initial state is set to an isothermal unstable region, according to the equation of state, the system will automatically separates to the liquid phase and the vapor phase and then achieve equilibrium condition.

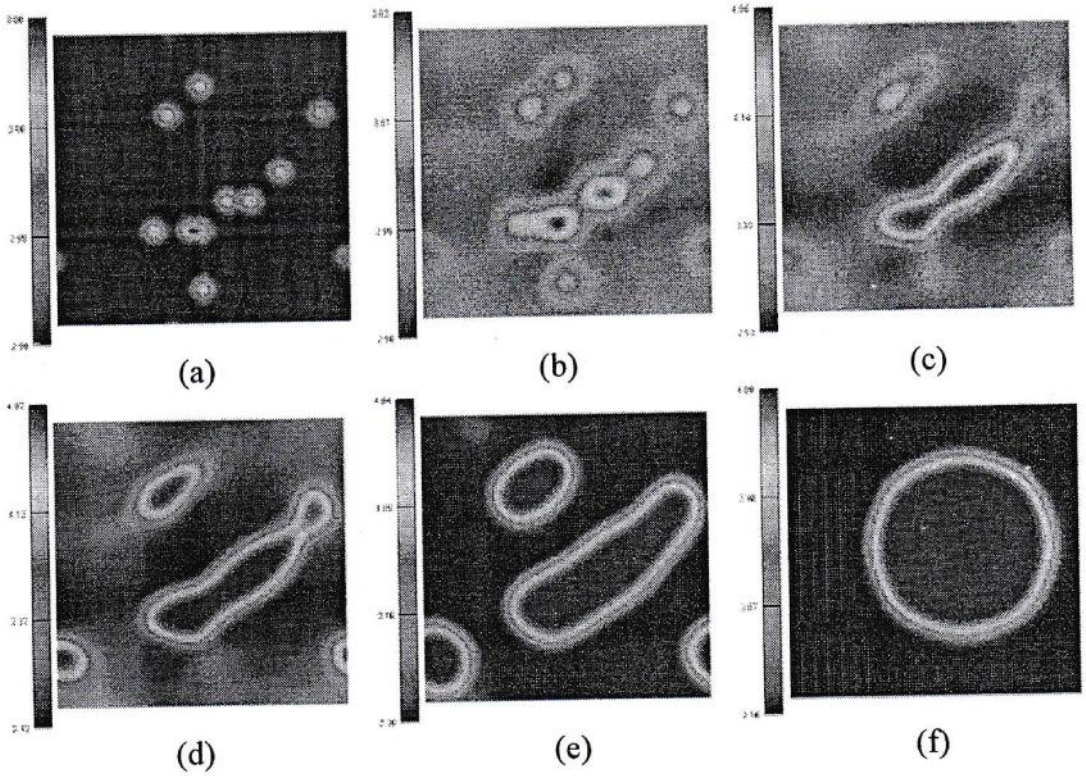

Figure 3: Snapshot of phase separation

The transient behavior of phase separation was done in order to examine the validity of Yonetsu's model. The D2Q9 model with 101 × 101 lattice is used and the simulation was done at $T = 0.55$. Other parameters are presented in the Table 1.

Table 1: Parameters used for the simulation of phase separation

Δx	Δy	Δt	τ	κ
0.05	0.05	0.01	1.00	0.0001

Figure 3 shows the domain morphology at time steps of 200, 800, 2400, 2700, 3300 and 8000 separately. Although the initial bubble nuclei are small, the mass densities inside the droplets are close to their equilibrium value, as illustrated in Figure 3(a). The small bubbles are coalescing and form larger and larger bubbles as the time evolves. Figure 3(b) contains coalescing bubbles in the view field. A spherical bubble at equilibrium state is illustrated in Figure 3(f). The interface during the system evolution is clear and of the same thickness.

3.2 Bubble Rise

In this section, the two-dimensional single bubble rising under buoyancy is simulated. The density of each phase are taken as $\rho_L = 4.895$and $\rho_G = 2.221$. The periodic boundary condition is employed at all boundaries. Initially, it is located at the lower region (one sixth of the height) of computational domain of 481 × 161. The dimensionless parameters (Eotvos, Morton number and Reynolds) are defined as

$$Eo = \frac{g\Delta\rho d^2}{\sigma} \tag{31}$$

$$Mo = \frac{g\rho_L \Delta\rho \upsilon^4}{\sigma^3} \tag{32}$$

$$\mathrm{Re} = \frac{Ud}{\upsilon} \tag{33}$$

where g is the gravitational force, $\Delta\rho$ is the density difference for two phase system, ρ_L is the fluid density, U is the velocity of the bubble at equilibrium state, d is the radius of bubble and σ is the surface tension coefficient.

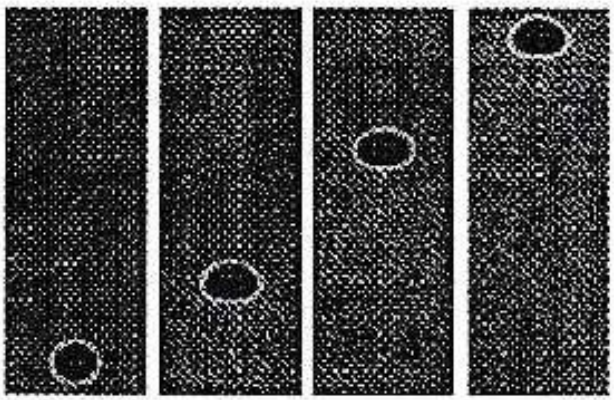

Figure 4: Time evolution of bubble rise phenomenon at $Eo = 10$

Simulations have been done for Eo of 10 and 20. Due to buoyancy force, the bubble will move upward. In the meantime, the middle part of the bubble will encounter a large deformation due to the hit of surrounding water. Equation 31 indicates that the increase of Eo is equivalent to the decrease of the surface tension coefficient σ. It is well known that the surface tension force is to resist the deformation of the bubble. In other words, the decrease of σ enhances the deformation of the bubble. This phenomenon is clearly revealed in Figure 4 and Figure 5 which display the bubble shape of the two cases. The bubble of case one is close to the original shape. As the Eo is increased, the bubble shape deformed. For the case of $Eo = 10$, the shape of the bubble does not change too much. This is because for this case, the surface tension force is strong, trying to keep its initial configuration. At $Eo = 20$, (Eo is increased and surface tension force decrease),

the bubble move up faster and the bubble's shape change. For all the cases, the bubble is always kept symmetrically.

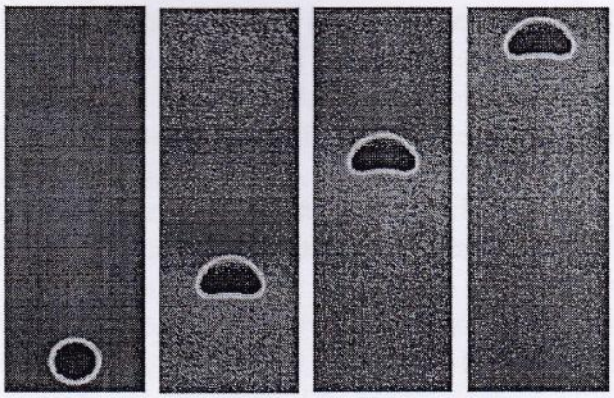

Figure 5: Time evolution of bubble rise phenomenon at $Eo = 20$

3.3 Bubbles Coalesce

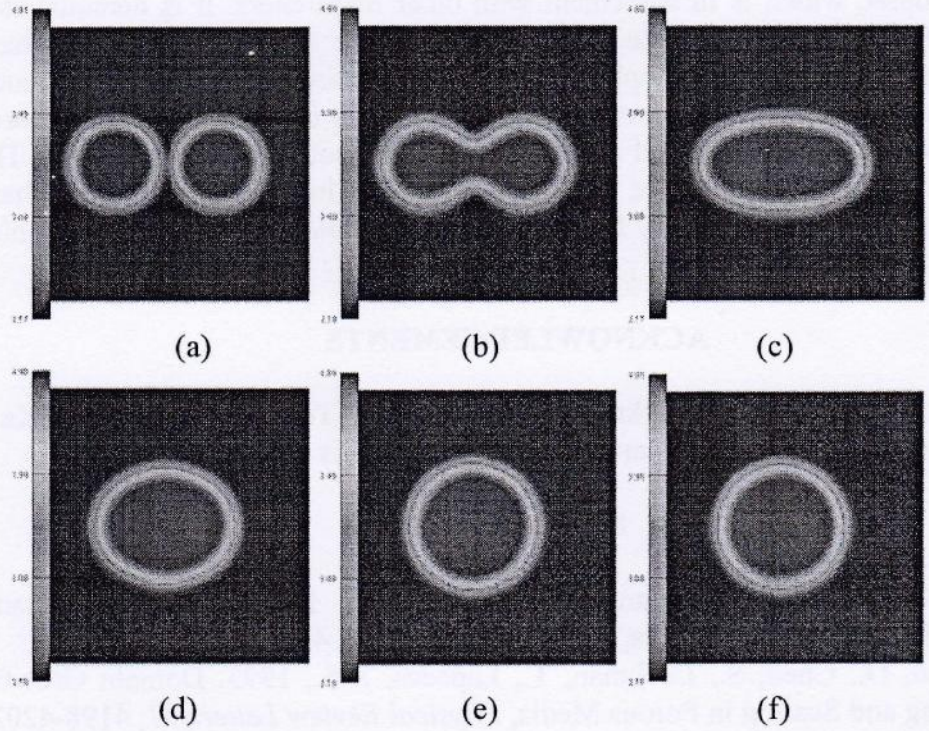

Figure 6: Snapshot of bubbles' coalesce

The bubble coalesces have been study in details by Zheng et al. [12]. Zheng found that for the two stationary bubbles without collision, it was found that the distance (gap) between the bubbles and the interface width (w) are the major factors to decide whether the two bubbles will coalesce or not. When the gap of the two bubbles is larger than $2w$, the two bubbles will not coalesce. Otherwise, they will coalesce.

To study the effect of the width of interface layer on the numerical results, two stationary bubbles without collision is considered as shown in Figure 6. The computational domain is taken as 100×100. Initially, two circular bubbles with the radius R are located horizontally with a gap of d. The periodic boundary condition is employed at all boundaries. The density ratio is set as 2.214. The parameters are chosen as $R = 15$ lattice units and $\tau = 1.00$. The gap of the two bubbles (d) is taken as 0.8, while the width of the interface (w) is 1.8 lattice units.

Numerical results are shown in Figure 6. It can be easily observed that for the case where the gap of two bubbles is less than $2w$, the two bubbles coalesce eventually without collision and are in agreement with other researcher's results.

4.0 CONCLUSIONS

This paper has shown the capabilities of lattice Boltzmann method in solving the two-phase system. The advantages of multiphase lattice Boltzmann approach are not only capable of incorporating interface deformation and interaction but also the interparticle interactions, which are difficult to implement in traditional methods. Two-phase flow benchmark tests showed the relaxation process of the bubble/droplet, which is in agreement with other researchers. It is demonstrated that the free energy two-phase LBE model has the ability to simulate phase separation, bubble rise and droplets coalesce. The phase separation phenomenon has been correctly predicted where the value of density or volume for both phases at equilibrium state are in good agreement with the isothermal $p - V$ graph. The numerical results of bubble rise and droplet coalesce indicate that the two-phase lattice Boltzmann schemes may be applicable for simulating interfacial dynamics in immiscible phases.

ACKNOWLEDGEMENTS

The authors would like to acknowledge Universiti Teknologi Malaysia, Keio University and Malaysia Government for supporting this research.

REFERENCES

1. Gunstensen, A.K., Rothman, D.H., Zaleski, G., 1991. Lattice Boltzmann Model for Immiscible Fluids, *Physics Review A 43*, 4320-4327.
2. Grunau, D., Chen, S., Lookman, T., Lapedes, A.S., 1993. Domain Growth, Wetting and Scaling in Porous Media, *Physical Review Letters 71*, 4198-4202.
3. Boghosian, B.M., Coveney, P.V., 2000. Particulate Basis for an Immiscible Lattice-gas Model, *Computer Physic Communication 129*, 46-55.
4. Shan, X., Chen, H., 1993. Lattice Boltzmann Model for Simulating Flows with Multiple Phases and Components, *Physical Review E 47*, 1815-1820.
5. Martys, N.S., Douglas, J.F., 2001. Critical Properties and Phase Separation in Lattice Boltzmann Fluid Mixtures, *Physical Review E 63*, 031205/1-031205/18.
6. Hazi, G., Imre, A.R., Mayer, G., Farkas, I., 2002. Lattice Boltzmann Method for Two-Phase Flow Modelling, *Annals of Nuclear Energy 29*, 1421-1453.

7. Swift, M.R., Osborn, W.R., Yeoman, J.M., 1995. Lattice Boltzmann Simulation of Nonidela Fluids, *Physical Review Letters 75*, 830-833.
8. Holdych, D.J., Geogiadis, J.G., Buckius, R.O., 2001. Migration of a Van Der Waals Bubbles: Lattice Boltzmann Formulation, *Physics of Fluids 13*, 817-825.
9. Yonetsu, H., 2003. *2-Dimensional Simulation of Two-Phase Flow using Discrete Boltzmann Equation*, MSc Thesis, Keio University, Japan.
10. Bhatnagar, P.L., Gross, E.P., Krook, M., 1954. A Model for Collision Proces in Gasses, *Physical Review 94*, 511-525.
11. Yang, Z.L., Dinh, T.N., Nourgeliev, R.R., Sehgal, B.R., 2001. Numerical Investigation of Boiling Regime Transition Mechanism by a Lattice Boltzmann Model, *Nuclear Engineering and Design 204*, 143-153.
12. Zheng, H.W., Shu, C., Chew, Y.T., 2005. Lattice Boltzmann Interface Capturing Method for Incompressible Flows, *Physical Review E 72*, 056705-056715.